Proc. 2002 Australasian Conference on Robotics and Automation
Auckland, 27-29 November 2002

Six-Dimensional Visualisation of End-Effector Pose Using Colour Spaces

Joshua D. Petitt
School of Mechanical Engineering
The University of Western Australia
35 Stirling Highway, Crawley, WA 6009.
petitj01@mech.uwa.edu.au

Karol Miller
School of Mechanical Engineering
The University of Western Australia
35 Stirling Highway, Crawley, WA 6009.
kmiller@mech.uwa.edu.au

Abstract

This paper discusses methods for visualising the workspace of a generic robot using the colour space to indicate orientation and dexterity of the tool. A method is shown to convert Euler angles into a RGB colour representation. An alternative method for examining generic workspace quality based on dexiterity is also shown. These methods are then applied to selected examples.

1 Introduction

Visualisation tools have become an important commodity with the advent of computer-aided engineering. This is especially true in the field of robotics, where the marriage of computer and mechanism yields a machine whose capabilities in certain areas outstrips those of its designers. However, before the robot ever becomes a physical entity, the design is carefully scrutinized. In this phase of the design cycle, visualisation of the digital representation becomes important.

The focus of this paper is the visualisation of a generic manipulator workspace. The workspace will be defined as the volume defined by every pose which the end-effector can achieve. Some researchers [Singh and Rastegar, 1995] make the important distinction between workspace assembly modes, however this paper will concentrated on the total workspace which is the union each assembly mode sub-workspace. Therefore, for *n* assembly modes, the total workspace Ω_{total} is

$$\Omega_{total} = \bigcup_{i=0}^{n} \Omega_i \tag{1}$$

The tool pose represents both position and orientation. The orientation of the end-effector can be represented in many different ways including rotation matrices, Euler angles, quaternions, and Plücker coordinates. In this discussion, only rotation matrices and Euler angles will be addressed. [Merlet, 2000] states that for a six-dimensional workspace "there is no possible graphical illustration". While that statement is partially correct, the goal of this paper is to show that using common techniques found in computer graphics, it is possible to represent *six dimensions* based on the visualisation method. The methods are especially useful when dealing with interactive two-dimensional images, such as those producible on the computer screen, where the point of view can be manipulated.

2 Representing Orientation

2.1 Transformation Matrices

The use of homogenous transformation matrices has become prevalent in the robotics community, especially in the area of serial manipulators. A transformation matrix can be represented by

$$\mathbf{T} = \begin{bmatrix} \mathbf{R} & \mathbf{d} \\ \mathbf{0} & 1 \end{bmatrix} \tag{2}$$

The orientation component, $\mathbf{R}$, is a 3x3 matrix representing the projections of the local coordinate system onto the global coordinate system.

2.2 Euler Angles

Euler angles are often used in the field of robots to describe the orientation of the end-effector. Despite their drawbacks, which include ambiguity between multiple definitions and the ability to represent the same orientation with two or more (possibly infinite) combinations of Euler angles, they still remain popular probably because of the ease of geometric interpretation. The form of Euler angles that will be used here are $[\theta\ \phi\ \psi]$ which correspond to a rotation about the *z*-axis, followed by a rotation about the *x*-axis, and finally another rotation about the *z*-axis. This series of rotations to define orientation is called the *x convention*. The angles have a range of

$$\theta = [0, 2\pi) \tag{3}$$

$$\phi = [0, \pi) \tag{4}$$

$$\psi = [0, 2\pi) \tag{5}$$

3 Colour Spaces

A brief overview of colour spaces will be given to familiarize the reader with the concepts and definitions needed for later discussion, for more information on the subject an excellent introduction is given in [Foley et al., 1994]. The three common colour spaces are RGB, CMY, and HSV.

The RGB colour space defines a cartesian coordinate system whose the primary axes are the **r**ed, **g**reen and **b**lue components of colour. Each axis ranges from zero to unity, therefore the entire space lies in a unit cube.

The CMY colour space, which stands for **c**yan-**m**agenta-**y**ellow, also defines a cartesian coordinate system and is closely related to the RGB colour space by the following transformation

$$\begin{bmatrix} C \\ M \\ Y \end{bmatrix} = \begin{bmatrix} 1 \\ 1 \\ 1 \end{bmatrix} - \begin{bmatrix} R \\ G \\ B \end{bmatrix} \tag{6}$$

The final colour space, HSV which stands for **h**ue-**s**aturation-**v**alue, defines a cylindrical coordinate system where $[H\ S\ V]$ correspond to $[r\ \theta\ z]$ in the standard cylindrical coordinate system. The colour space is a subset of the coordinate system defined by a hexcone.

The important observation is that each colour space is described by three independent variables, thus three independent parameters at any position in space can be encoded as a specific colour. Because orientation can be represented by three parameters, Euler angles, the tool pose can be completely described at any point in space.

For the planar situation, only three variables need to be represented to describe the tool pose, two for position and one for orientation. Thus, a gray scale representation can be used to encode the angle of rotation.

4 Visualisation of Orientation

4.1 Rotation Matrices to RGB

Each of the local coordinate axis vectors in the orientation matrix, $\mathbf{R}$, can be mapped into colour space. Note that since each of the vectors has a magnitude of unity, only a subset of the colour space is used, more precisely, only the colours lying on a sphere. If the cartesian colour spaces are used for representation, the vectors must first be scaled and shifted. Because the axes of the cartesian colour spaces are bounded between zero and unity, an appropriate equation to describe the mapping would be

$$f(\mathbf{R}) = \frac{1 + \mathbf{R}}{2} \tag{7}$$

This is a one to one mapping which shifts the origin to the center of the colour space, and reduces the vector length by half. It should be noted that only two of the three vectors are needed since the other is implicitly defined by the other two.

This method of encoding orientation has the advantage that pure white [1,1,1] or pure black [0,0,0] are not possible colours. This allows easy differentiation between the information colours and the background colour in a user interface. It often also leads to pleasing colour combinations. However, the main drawback is that three colours are needed for encoding the orientation; it would be most desirable that one colour define an orientation.

4.2 Euler Angles to RGB

Perhaps the most straightforward representation of orientation is the conversion of Euler angles to the RGB colour space. By scaling the angles $[\theta\ \phi\ \psi]$ by $\left[\frac{1}{2\pi}\ \frac{1}{\pi}\ \frac{1}{2\pi}\right]$, a three-element vector with values ranging from zero to unity is obtained, thus covering the entire colour space. This vector directly corresponds a location in the RGB colour space. An advantage to the colour space representation of orientation is that it removes the ambiguities from the Euler angles (more than one angle combination, and therefore colour, can represent the same orientation).

4.3 Examples of Orientation Visualisation

Three configurations of planar two degree-of-freedom robots are now analyzed to demonstrate the concept of orientation encoding. These are the prismatic-prismatic, the revolute-prismatic, and revolute-revolute manipulators shown in Figure 1.

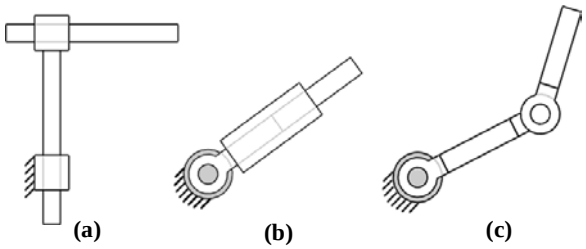

Figure 1 - Two DOF manipulators (a) prismatic-prismatic (b) revolute-prismatic (c) revolute-revolute

Note that each of these manipulators only has two degrees of freedom, so the position and orientation of the end-effector are not independent.

Prismatic-prismatic manipulator

This robot configuration operates in a cartesian configuration. Because the orientation of the end-effector does not vary as the joints are actuated, the solution to the prismatic-prismatic manipulator is trivial. Note that the orientation of the end-effector could be chosen to be any angle with respect to the global coordinate system, therefore any associated grayscale colour could be used. Black was chosen for convenience and that it corresponds to zero radians. The important aspect of Figure 2 is that the orientation is constant throughout the workspace.

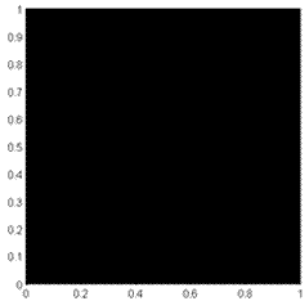

Figure 2 - Prismatic-prismatic orientation work-space

Revolute-prismatic manipulator

The second two degree of freedom manipulator to be examined is the revolute-prismatic manipulator. This manipulator operates in a cylindrical coordinate system, thus the angle of the first joint determines the angle of the end-effector. The workspace of this manipulator is show in Figure 3.

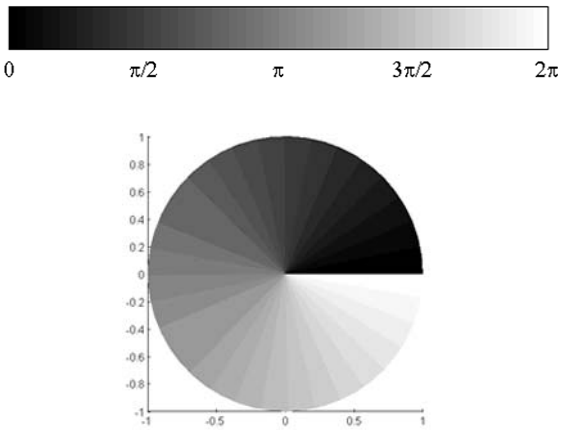

Figure 3 - Revolute-prismatic workspace

Revolute-revolute manipulator

The final two degree of freedom manipulator is the revolute-revolute type. This manipulator has a workspace shown in Figure 4a. Note that this workspace was created with equal lengths for each arm. If the lengths had been unequal, this would produce workspaces similar to those shown in Figures 4b and 4c.

Another issue with the revolute-revolute manipulator, which is also relevant to manipulators with higher degrees of freedom, is the issue of modality, or the assembly mode of the robot. Notice that the cartesian and spherical manipulators have only one mode of assembly for any location in the workspace. The revolute-revolute manipulator has two modes of assembly.

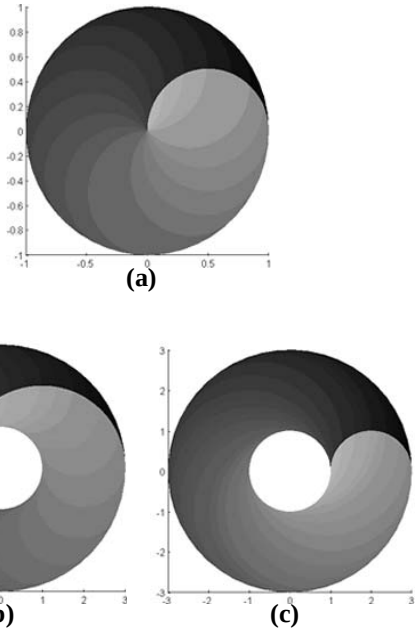

Figure 4 - Revolute-revolute workspace with (a) 1:1 (b) 1:2 (c) 2:1 link proportions

5 Visualisation of Dexterity

Dexterity can be thought of as proportional to all the orientations a robot can achieve at a specific position in space. This is equivalent to the volume of achievable points in orientation space, which for the Euler angle orientation space the maximum volume is $4\pi^3$.

The calculation of the workspace can be done with various methods [Cwiakala and Lee, 1985; Kohli and Spanos, 1985; Rastegar and Fardanesh, 1990; Merlet, 2000]. The method used here is a discretation of the workspace whereby at each location (position and orientation), the inverse kinematic constraints of the manipulator are checked. If the robot does not violate the constraint equations, then the point is considered within the workspace. This method, while elementary in approach, is considered by the author to be superior to other methods including geometric [Merlet, 2000] and probabilistic methods [Rastegar and Fardanesh, 1990] for this application. The primary reason for this opinion is that the maximal reach of the workspace is of secondary importance to the overall quality throughout the workspace. Therefore points in the interior of the workspace must also be evaluated.

The notation used for the inverse kinematics of the manipulator is taken from [Jalon and Bayo, 1994] and is consistent with the conventional symbols used by many others. The nonlinear constraint equations of the mechanism are expressed as a function of the joint variables, $\Phi(\mathbf{q})$. If the mechanism assembles at a specific location then the constraint equations will be equal to a zero vector, mathematically expressed as

$$\Phi(\mathbf{q}) = \mathbf{0} \qquad (8)$$

If the constraint equations are not satisfied then the right-hand side of the equation represents the residual error. For the inverse kinematic problem, the inverse constraint equations are a function of tool location. The equation for the inverse constraint equations can be written as

$$\Phi^{-1}(\mathbf{X}) \tag{9}$$

Because the workspace is discretized, each node is assumed to represent a volume. The volume calculation of the orientation space is then equivalent to the numerical integration of the workspace, which could be mathematically stated as

$$C_{x,y,z} = \sum_{i=1}^{n} c(\mathbf{X}) \tag{10}$$

where

$$c(\mathbf{X}) = \begin{cases} \frac{1}{n} & \text{if } \Phi^{-1}(\mathbf{X}) = 0 \\ 0 & \text{otherwise} \end{cases} \tag{11}$$

5.1 Applications for Workspace Visualisation

Three DOF Parallel Manipulator

The three degree planar parallel manipulator, shown in Figure 5, has been studied by [Gosselin and Merlet, 1994; Sefrioui and Gosselin, 1995] for both direct kinematics and singularity analysis. The distinction between the three DOF planar mechanism compared to the first three manipulators is that at any point a number of poses may be achieved. The workspace boundary for the manipulator is shown in [Sefrioui and Gosselin, 1995] with a plot of the singularity loci under different parameters of the mechanism. Of more practical interest, from a design standpoint, is not where the mechanism loses controllability (i.e. near singular positions), but where controllability is high. Because a robot could be described as a "general purpose mechanism", one would desire it to be able to achieve a large range of poses. The placement of the robot is also of particular importance for task performance.

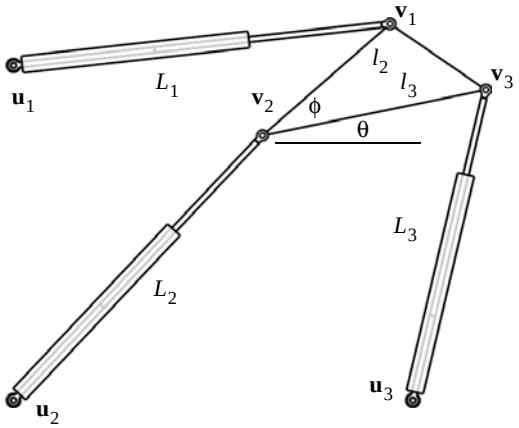

Figure 5 - Three DOF Parallel Manipulator

The constraint equations for the three DOF planar mechanism are

$$\Phi^{-1} = \begin{cases} \|\mathbf{u}_1 - \mathbf{v}_1\| - L_1 \\ \|\mathbf{u}_2 - \mathbf{v}_2\| - L_2 \\ \|\mathbf{u}_3 - \mathbf{v}_3\| - L_3 \end{cases} \tag{12}$$

where

$$\mathbf{v}_1 = l_2 \begin{bmatrix} \cos(\theta + \phi) \\ \sin(\theta + \phi) \end{bmatrix} + \mathbf{v}_2 \tag{13}$$

$$\mathbf{v}_3 = l_3 \begin{bmatrix} \cos\theta \\ \sin\theta \end{bmatrix} + \mathbf{v}_2 \tag{14}$$

For this example, $\mathbf{u}_1 = [0, 6]$, $\mathbf{u}_2 = [0, 0]$, $\mathbf{u}_3 = [7, 0]$, $l_2 = 3$, $l_3 = 4$, $\phi = \pi/6$, $L_{min} = 6$ and $L_{max} = 14$. Figure 7 illustrates the constant orientation workspaces for the 3 DOF planar parallel manipulator. From these diagrams, one might reason that the workspace of the manipulator was relatively large. However, when these are compared to Figure 6, the combined workspace plot, one can observed that there is only a small region of high manipulability (the black area in the upper right corner). In only this region, could the manipulator perform a generic task. In all other regions, the placement of the manipulator with respect to the task becomes a prime importance in the ability of the robot to perform its duties.

Figure 6 - Workspace for Three DOF Parallel Manipulator

[Singh and Rastegar, 1995] have suggested a global conditioning index, based on the condition number of the Jacobian, evaluated over the manipulator workspace to determine the global manipulability. The author believes that this method is a valid approach which yields insight into workspace quality, however the calculation of the Jacobian matrix at each pose is computationally expensive, often more so than the inverse kinematic constraints. Thus, the method presented here is an alternative method for determining workspace quality, and more importantly determining areas within the workspace which are of best quality.

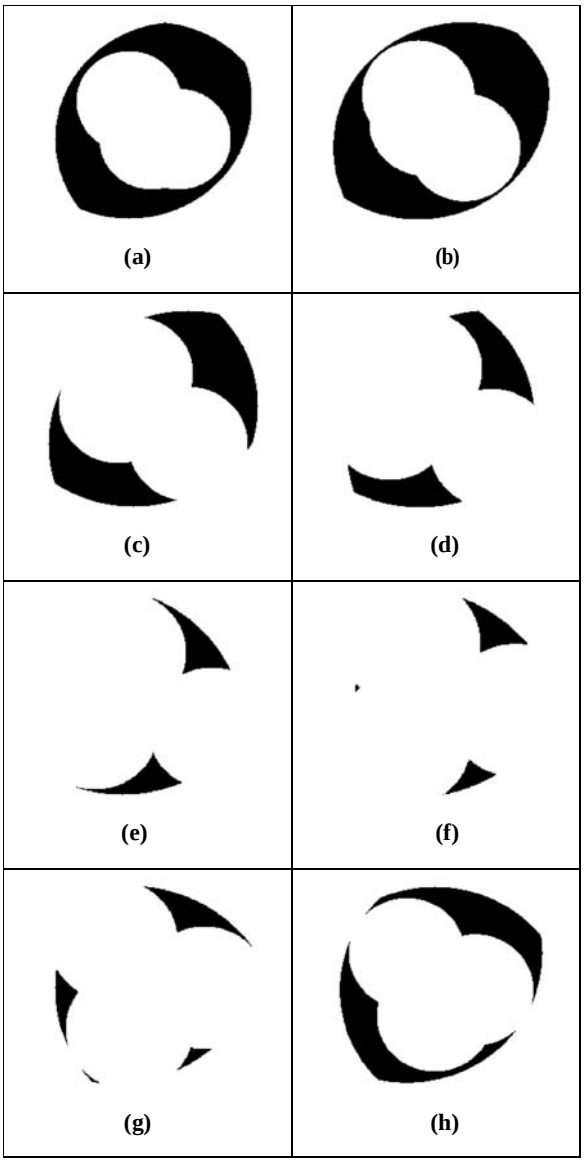

Figure 7 - Constant Orientation Workspaces for Three DOF Parallel Manipulator at (a) 0 (b) 1/4 π (c) 1/2 π (d) 3/4 π (e) π (f) 5/4 π (g) 3/2 π (h) 7/4 π

Six Degree of Freedom Manipulator

The approach taken for the three degree of freedom planar manipulator can now be directly extended to the six dimensional case. This will yield a final colour value for each point that allows the designer to quickly observe the quality of the workspace. Areas with higher manipulability will be lighter than those with less manipulability. One drawback to this method is that it is not immediately evident if the manipulator can achieve any particular orientation at a specified location. Thus, an alternative is to resort to the constant orientation workspace used in [Merlet, 2000].

The manipulator which examined is a special configuration of the Stewart platform which [Merlet, 2000] refers to as an MSSM configuration, shown in Figure 8.

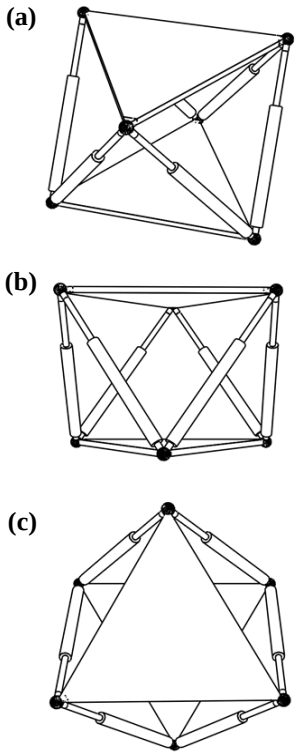

Figure 8 - MSSM six DOF parallel robot (a) isometric (b) front and (c) top views

An isometric view of the workspace is shown in Figure 9. This workspace was generated with a grid size of 0.05 for spacial resolution and a resolution of $\pi/8$ for each of the Euler angles. Therefore at each point, 2048 different orientations were tested. One will observe from Figure 10 that the workspace is highly dependent on the orientation of the travelling plate. This is also illustrated in Figures 11 and 12 which show that in the regions of highest dexterity, only ~8% of orientations are possible.

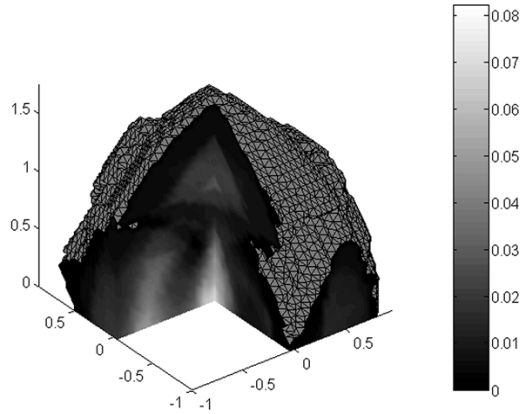

Figure 9 - Cutaway Isometric view of MSSM workspace

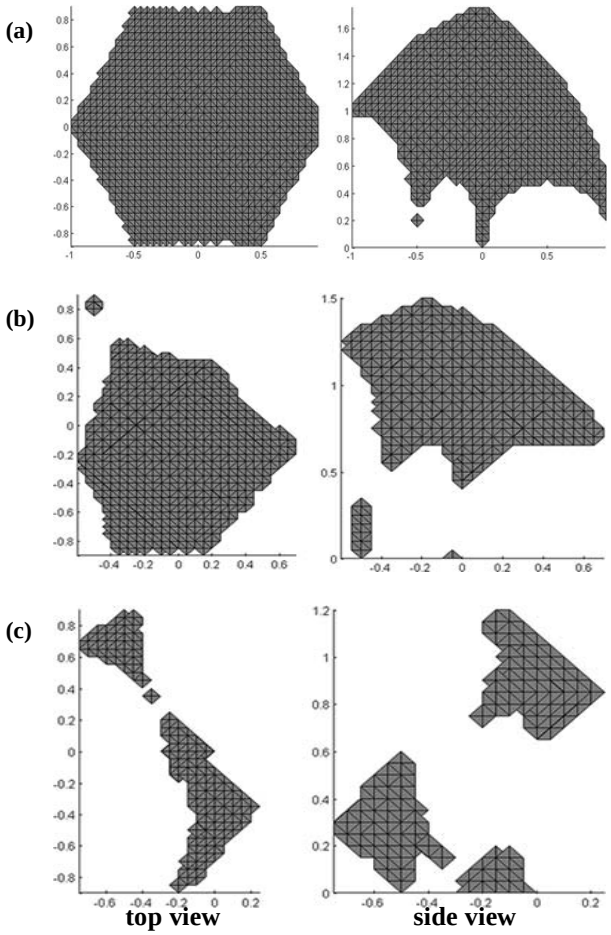

Figure 10 - Constant orientation workspace for MSSM manipulator at (a) [0,0,0] (b) [0,π/8,0] and (c) [0,π/4,0]

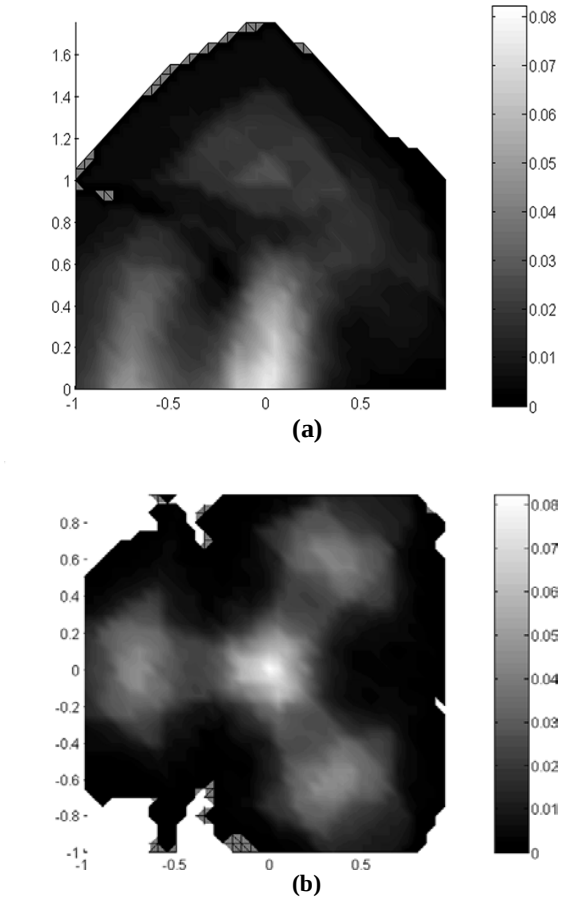

Figure 11 - (a) side and (b) top views of MSSM workspace

6 Conclusion

Methods for visualisation of a manipulator workspace which utilize colour for conveying information on orientation and dexterity have been presented. These methods were applied to simple planar manipulators as well as three and six degree of freedom examples. From this, one could conclude that colour is an effective means for visualisation of manipulator workspaces.

References

[Cwiakala and Lee, 1985] Cwiakala, M. and T. W. Lee (1985). "Generation and Evaluation of a Manipulator Workspace Based on Optimum Path Search." Journal of Mechanisms, Transmissions, and Automation in Design **107**: 245-255.

[Foley et al., 1994] Foley, J. D. et al. (1994). Introduction to Computer Graphics, Addison-Wesley Publishing.

[Gosselin and Merlet, 1994] Gosselin, C. M. and J.-P. Merlet (1994). "The Direct Kinematics of Planar Parallel Manipulators: Special Architectures and Number of Solutions." Mech. Mach. Theory **29**(8): 1083-1097.

[Jalon and Bayo, 1994] Jalon, J. G. d. and E. Bayo (1994). Kinematic and Dynamic Simulation of Multibody Systems. New York, Springer-Verlag.

[Kohli and Spanos, 1985] Kohli, D. and J. Spanos (1985). "Workspace Analysis of Mechanical Manipulators Using Polynomial Discriminants." ASME Journal of Mechanisms, Transmissons, and Automation in Design **107**: 209-215.

[Merlet, 2000] Merlet, J.-P. (2000). Parallel Robots, Kluwer.

[Sefrioui and Gosselin, 1995] Sefrioui, J. and C. M. Gosselin (1995). "On the Quadratic Nature of the Singularity Curves of Planar Three-Degree-of-Freedom Parallel Manipulators." Mech. Mach. Theory **30**(4): 533-551.

[Singh and Rastegar, 1995] Singh, J. R. and J. Rastegar (1995). "Optimal Synthesis of Robot Manipulators Based on Global Kinematic Parameters." Mech. Mach. Theory **30**(4): 569-580.

[Rastegar and Fardanesh, 1990] Rastegar, J. and B. Fardanesh (1990). "Manipulator Workspace Analysis Using the Monte Carlo Method." Mech. Mach. Theory **25**(2): 233-239.